

ChemComm

Accepted Manuscript



This is an *Accepted Manuscript*, which has been through the Royal Society of Chemistry peer review process and has been accepted for publication.

Accepted Manuscripts are published online shortly after acceptance, before technical editing, formatting and proof reading. Using this free service, authors can make their results available to the community, in citable form, before we publish the edited article. We will replace this *Accepted Manuscript* with the edited and formatted *Advance Article* as soon as it is available.

You can find more information about *Accepted Manuscripts* in the [Information for Authors](#).

Please note that technical editing may introduce minor changes to the text and/or graphics, which may alter content. The journal's standard [Terms & Conditions](#) and the [Ethical guidelines](#) still apply. In no event shall the Royal Society of Chemistry be held responsible for any errors or omissions in this *Accepted Manuscript* or any consequences arising from the use of any information it contains.

Cite this: DOI: 10.1039/c0xx00000x

www.rsc.org/xxxxxx

COMMUNICATION

Inherent anchorage in UiO-66 nanoparticles for efficient capture of alendronate and its mediated release

Xiangyang Zhu, Jinlou Gu,* Yao Wang, Bing Li, Yongsheng Li, Wenru Zhao, and Jianlin Shi*

Received (in XXX, XXX) Xth XXXXXXXXX 20XX, Accepted Xth XXXXXXXXX 20XX

DOI: 10.1039/b000000x

Zr-based MOF nanoparticles were applied as an efficient carrier for alendronate delivery, and an unprecedented drug loading capacity was achieved thanks to the inherent drug anchorages of Zr-O clusters therein. The encapsulated drug featured with a pH-dependent release profile, and inhibited the growth of cancer cells more efficiently than free drug.

The amino-bisphosphonate of alendronate (AL) is widely used for the treatment of osteoporosis, solid tumor bone metastases and myeloma bone disease.¹ Although AL is mostly known for its strong anti-resorptive activity, it also demonstrates direct or indirect antitumor effects, notably in the cases of prostate and breast cancers.² However, its short lifetime and preferential accumulation within bone tissues limit its use as antitumor agents for extra-skeletal malignancies.³ Furthermore, due to its poor bioavailability, administration of over-high doses is usually required for practical clinical applications, which will inevitably cause systemic toxicity. Therefore, a local, sustained AL delivery system that can enhance the loading capacity and delivery efficiency of AL into cancer cells is highly desirable.

It has been well documented that some metal oxides, such as zirconia, can be modified with phosphonates due to the stable M-O-P bonds.⁴ Thus, introducing metal oxide into nanocarriers was strategically employed to serve as the drug anchorage for AL capture. For example, Colilla and co-workers^{1a} modified the framework of mesoporous silica with zirconia, which not only effectively increased AL loading amount but also mediated its release. However, limited by the small amount of the doped metal oxide, the AL loading capacity was still relatively low.

Porous metal-organic frameworks (MOFs) have been successfully employed as drug delivery vehicles attributing to their enormous porosity, high surface area and versatile framework compositions.⁵ Several studies confirmed that MOFs exhibited exceptional biocompatibility and biodegradability.⁶ However, their relatively low chemical and thermal stabilities could be the key limitations to meet the requirements of practical applications.⁷ Recently, zirconium based MOFs of UiO-66 received great attention due to its excellent stabilities.⁸ UiO-66 contains linear 1,4-benzenedicarboxylate (BDC) ligand and $Zr_6O_4(OH)_4$ clusters as 12-connected nodes.⁹ It possesses a face-centered-cubic arrangement of the Zr-O clusters and thus consists of octahedral (~ 11 Å) and tetrahedral (~ 8 Å) cages in 1:2 ratio.¹⁰ These open cavities and Zr-O clusters make it possible to tailor the controlled capture and release of AL molecules based on the

strong complexation of Zr-O-P bonds. These features coupled with its non-toxic nature and easiness for nanoparticle formation¹¹ make UiO-66 an ideal candidate for AL delivery.

Herein, UiO-66 nanoparticles (NPs) with uniform particle size were elaborated and successfully applied as an AL delivery vehicle. To the best of our knowledge, this is the first report on taking advantage of the Zr-O clusters in UiO-66 as natural drug anchorages to realize the effective capture of AL molecules. The AL loading amount was unprecedentedly high up to 1.06 g of drug per gram UiO-66, and their release from the nanocarriers was greatly sustained and featured with a pH-dependent profile. The obtained NPs exhibited remarkable water dispersity, and could be effectively endocytosized by cancer cells. The encapsulated drug presented enhanced growth inhibition effect than free AL against both MCF-7 and HepG2 cells.

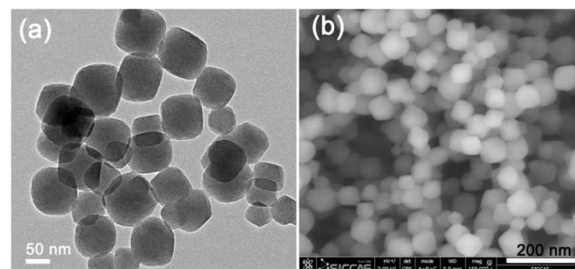


Fig. 1 Typical (a) TEM and (b) FE-SEM images of the synthesized UiO-66 nanoparticles.

The highly crystallized UiO-66 NPs were prepared by a modified solvothermal method (See ESI†).⁸ TEM was used to investigate their size and morphology. It can be observed that the monodispersed nanocrystals with a mean diameter of *ca.* 70 nm are mainly cubical in shape (Fig. 1a). FE-SEM further confirms that the isolated UiO-66 crystals with cubical morphology and a diameter range from 50 to 90 nm were obtained (Fig. 1b). This size matches well with the reported suitable nanoparticle diameter for the effective cell uptake.^{5c} Hence, it is anticipated that the obtained UiO-66 NPs could be internalized into cells effectively. Actually, the particle size of UiO-66 NPs could be also determined by dynamic light scattering (DLS) technique thanks to their well water dispersity. The hydrodynamic size is narrowly distributed and peaks at *ca.* 100 nm (Fig. S1, ESI†), which is slightly larger than the geometric size obtained by either TEM or SEM. When a laser pointer was used to illuminate the NPs

suspension, Tyndall phenomenon can be clearly recognized in agreement with the DLS analysis (Inset of Fig. S1, ESI†).

X-ray diffraction (XRD) technique was employed to characterize the structural evolution of the synthesized UiO-66 and AL loaded UiO-66 (AL-UiO-66). The similar Bragg diffraction peaks of both samples indicate that the AL loading did not alter the parent crystalline structure of UiO-66 (Fig. S2, ESI†). A significant decrease in the peak relative intensity is observed for AL-UiO-66, which could be ascribed to the trapping of the AL in the UiO-66 pores and consequently results in the decreased X-ray contrast between porous framework and pore cages. The AL encapsulation did not change the morphology of nanocarriers as shown by TEM and SEM (Fig. S3a and S3b, ESI†).

Table 1. Texture parameters of UiO-66 and AL-UiO-66

Samples	$S_{\text{BET}}(\text{m}^2 \text{g}^{-1})$	$V_{\text{P}}(\text{cm}^3 \text{g}^{-1})$
UiO-66	1136	0.63
AL-UiO-66	45	0.07

The variations of surface area and pore volume of UiO-66 upon drug loading were analyzed by nitrogen sorption techniques. Both samples before and after drug loading display typical type-I gas sorption isotherms (Fig. S4, ESI†). This agrees well with the fact that the AL loading process did not destroy the structure integrity of UiO-66. AL-UiO-66 exhibits a BET surface area of $45 \text{ m}^2 \text{g}^{-1}$, which is much lower than that of pristine UiO-66 ($1136 \text{ m}^2 \text{g}^{-1}$, Table 1) in accordance with an apparent change in the pore volume (from $0.63 \text{ cm}^3 \text{g}^{-1}$ to $0.07 \text{ cm}^3 \text{g}^{-1}$). The dramatic decreases in the surface area and pore volume can be attributed to the AL molecule bonding in the cages of UiO-66.

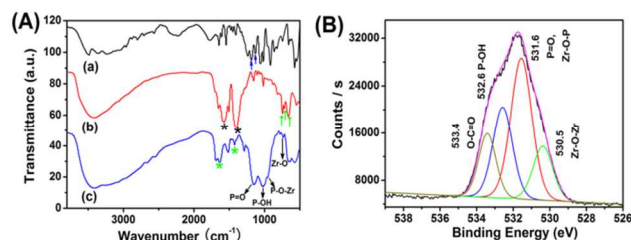


Fig. 2 (A) FT-IR spectra of (a) AL free drug, (b) parent UiO-66 nanocarriers and (c) AL loaded UiO-66. (B) The O1s XPS spectrum of AL-UiO-66.

The interaction of the UiO-66 framework with AL molecules was probed by Fourier transformed infrared (FT-IR) spectra (Fig. 2A). In the spectrum of pristine UiO-66, the intense doublet at 1590 and 1400 cm^{-1} (labeled with black stars) can be assigned to the in- and out-of-phases stretching modes of the carboxylate groups.⁸ The triplet at 723 , 650 and 550 cm^{-1} (labeled with green arrows) is attributed to Zr-O₂ as longitudinal and transverse modes, respectively.⁸ In contrast, after AL loading, the original bands at 1590 and 1400 cm^{-1} are blue-shifted to 1630 and 1433 cm^{-1} (labeled with green stars). Meanwhile, broad P-O stretching bands between 1200 and 900 cm^{-1} appear in the spectra of AL-UiO-66 with two main characteristic absorption bands at 1150 and 1020 cm^{-1} and a shoulder at 957 cm^{-1} . These bands, ascribing to the P=O, P-OH and P-O-Zr bonds, respectively, evidence that the drug has been successfully encapsulated into UiO-66.¹² We note that P-O bands in the AL molecule (labeled with blue arrows

in Fig. 2A) have been substantially red-shifted, which is plausible because binding of AL molecules to the Zr-O clusters could significantly decrease the frequency of the P-O stretching modes.¹² We also measured the XPS spectra of O, Zr and P of AL-UiO-66 to further confirm the existence of a linkage between UiO-66 and AL molecules (Fig. S5, ESI†). The deconvoluted O1s peak (Fig. 2B) consists of four peaks that are assigned to O in O-C=O (533.5 eV), P-O-H (532.6 eV), Zr-O-Zr (530.4 eV), and in Zr-O-P and P=O (531.6 eV), respectively.¹³ These strongly evidence that the Zr-O clusters in UiO-66 present high affinity towards AL molecules. Thanks to this strong complexation of Zr-O-P, the UiO-66 NPs show a remarkable AL loading capacity, which is extraordinarily high up to $51.4 \text{ wt}\%$, or 1.06 g of drug per gram of porous nanocarriers, as measured by ICP-AES. It should be pointed out that the loading amounts of AL in the reported nanocarriers in previous studies have never been higher than $37 \text{ wt}\%$,^{1b} revealing the overwhelming advantage of our strategy by employing UiO-66 as AL delivery vehicles.

The release of AL from UiO-66 NPs was assessed at $37 \text{ }^\circ\text{C}$ in PBS buffer with pHs of 5.5 and 7.4 (Fig. 3a). The time-dependent drug release profile is characterized by the slow and sustained patterns, which is quite beneficial to prevent the drug dissipation prior to reaching the cancer cells.^{5b} As shown in Fig. 3a, about 42.7% of AL is released from the UiO-66 NPs in 60 h at pH 7.4 , whereas more than 59% drug releases in the same time interval at pH 5.5 , indicative of the sensitivity of AL-UiO-66 to endosome/lysosome pH (*ca.* 5).¹⁴ The pH-responsive release feature may be attributed to the protonation of phosphate in the acidic environment, which weakens the interaction between AL and Zr-O cluster in UiO-66.¹⁴ These results imply that UiO-66 nanocarriers can diminish premature drug release during circulation but specifically enhance intracellular drug release, which will be definitely useful for effective tumor treatment.¹⁵ It is very interesting to note that the release amount was up to 88.1% in 108 h at pH 7.4 , while at pH 5.5 , the amount is less than 76% within the same time duration. Such a unique change in drug release behavior could be due to the lower degradation rate of UiO-66 in acidic condition than that in neutral and basic condition.⁸

To test *in vitro* cytotoxicity of the pristine UiO-66 NPs, cell viability was examined by standard MTT assays against HepG2 and MCF-7 cells (Fig. S6, ESI†). It was found that the changes in cell viability after 24 and 48 h of incubation were negligibly small. The cell proliferation is slightly hindered after incubation at a very high concentration up to $300 \text{ } \mu\text{g mL}^{-1}$ of nanocarrier for 48 h , indicating the relatively good biocompatibility of UiO-66 NPs *in vitro*.

Given the suitable particle size of UiO-66 nanocarriers, studies on the cellular uptake efficiency were carried out on HepG2 cells. We grafted fluorescent molecule of flavin mononucleotide (FMN, the phosphorylated form of vitamin B2) onto UiO-66 (UiO-66-FMN) by taking advantage of the high affinity between Zr-O clusters and phosphate function in FMN molecule for intracellular imaging.¹³ The effective capture of FMN on UiO-66 was verified by fluorescence measurement (Fig. S7, ESI†). To check whether FMN would leak from the nanocarrier, UiO-66-FMN was soaked in water for 24 h and the detached FMN was removed by centrifugation-redispersion cycles. The fluorescence

intensity of the resulting UiO-66-FMN was nearly the same as that of the sample before soaking (Fig. S8, ESI[†]), suggesting the leak was negligible in 24 h.

For flow cytometry analysis, the UiO-66-FMN suspension was incubated with HepG2 cells for 4 and 12 h. The percentage of cell population with log mean fluorescence intensity higher than 10^2 is more than 80% after 4 h incubation (Fig. S9, ESI[†]), while after 12 h incubation, only a slight increase in the fluorescence intensity in the same intensity area could be observed. This result illustrates that the nanocarriers can be easily endocytosized in the first 4 h incubation, and then the rate of cell uptake significantly decreased. To further verify that the as-synthesized nanocarriers could be efficiently endocytosized by cancer cells, confocal laser scanning microscopy (CLSM) analysis was carried out after incubation of UiO-66-FMN with HepG2 cells for 4 h. As shown in Fig. 3b, the NPs are remarkably internalized within a short period and distributed intensively in the cytoplasm as manifested by the appearance of green fluorescence around the nucleus in consistent with the results determined from flow cytometric analysis.

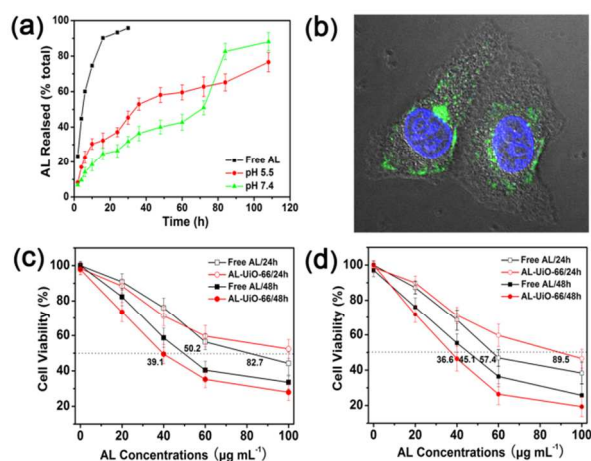


Fig. 3 (a) Free AL release profile from the dialysis bags at pH 7.4 (black) and the cumulative release profiles of AL from UiO-66 NPs in 5 mM PBS with pHs of 5.5 (red) and 7.4 (green) at 37 °C; (b) The merged confocal images of HepG2 cells after their incubation with $100 \mu\text{g mL}^{-1}$ UiO-66-FMN for 4 h at 37 °C; Cell viabilities of (c) HepG2 and (d) MCF-7 cells incubated with free AL and AL-UiO-66 at different concentrations for 24 and 48 h.

The therapeutic effect of AL loaded nanocarriers was studied through *in vitro* cytotoxicity measurements against MCF-7 and HepG2 cells using MTT method. The AL-UiO-66 exhibits slightly lower cytotoxicities than that of free AL with an equivalent dose in 24 h incubation for both cancer cells. This may be partially attributes to the different cell uptake processes between free AL and AL-UiO-66. Free AL can passively diffuse through the cell membrane and rapidly accumulate in the nucleus to kill the cancer cells, while the nanocarriers are generally endocytosized into the cells and detained in the endosomes instead of the cytoplasm.¹⁴ However, in 48 h of incubation, the AL-UiO-66 leads to higher amounts of cancer cell deaths than free AL. The IC_{50} values of AL-UiO-66 are much lower than those of free AL both in HepG2 (labeled in Fig. 3c) and MCF-7 (labeled in Fig. 3d) cell lines, implying the controlled release and enhanced growth inhibition effect of the encapsulated AL with

prolonged incubation time.

In summary, Zr-based MOF of UiO-66 NPs could be applied as an efficient carrier for AL delivery. The inherent Zr-O clusters in nanocarrier serve as natural drug anchorages for effective AL capture, leading to enhanced loading capacity and its mediated release. The pH-sensitive drug-carrier interaction accelerates the AL release in the acidic milieu of cancer cells, resulting in increased antitumor efficiency against both MCF-7 and HepG2 cell lines. These merits combined with its high stability, make UiO-66 highly promising for therapeutic applications as AL delivery vehicles.

This work was financially supported by the Natural Science Foundation of China (51072053, 51372084, 51132009), the Innovation Program of Shanghai Municipal Education Commission (13zz040) and the Nano-Special Foundation for Shanghai Committee of Science and Technology (12nm0502600).

Notes and references

Key Laboratory for Ultrafine Materials of Ministry of Education, School of Materials Science and Engineering, East China University of Science and Technology, Shanghai 200237, China. E-mail: jinlougu@ecust.edu.cn; Fax: +86-21-64250740; Tel: +86-21-64252599
[†]Electronic Supplementary Information (ESI) available: [Experimental details, DLS profile, XRD patterns, TEM and SEM, XPS, nitrogen adsorption-desorption data, fluorescence spectra, flow cytometric analyses and cytotoxicity data]. See DOI: 10.1039/b000000x/

- (a) M. Colilla, M. Manzano, I. Izquierdo-Barba, M. a. Vallet-Regí, C. Boissière and C. Sanchez, *Chem. Mater.*, 2010, **22**, 1821; (b) F. Balas, M. Manzano, P. Horcajada and M. Vallet-Regí, *J. Am. Chem. Soc.*, 2006, **128**, 8116.
- O. P. Varghese, W. Sun, J. n. Hilborn and D. A. Ossipov, *J. Am. Chem. Soc.*, 2009, **131**, 8781.
- K. Miller, C. Clementi, D. Polyak, A. Eldar-Boock, L. Benayoun, I. Barshack, Y. Shaked, G. Pasut and R. Satchi-Fainaro, *Biomaterials*, 2013, **34**, 3795.
- C. m. Queffelec, M. Petit, P. Janvier, D. A. Knight and B. Bujoli, *Chem. Rev.*, 2012, **112**, 3777.
- (a) D. Cunha, M. Ben Yahia, S. A. Hall, S. R. Miller, H. Chevreau, E. Elkaim, G. Maurin, P. Horcajada and C. Serre, *Chem. Mater.*, 2013, **25**, 2767; (b) C.-Y. Sun, C. Qin, X.-L. Wang, G.-S. Yang, K.-Z. Shao, Y.-Q. Lan, Z.-M. Su, P. Huang, C.-G. Wang and E.-B. Wang, *Dalton Trans.*, 2012, **41**, 6906; (c) K. M. Taylor-Pashow, J. D. Rocca, Z. Xie, S. Tran and W. Lin, *J. Am. Chem. Soc.*, 2009, **131**, 14261.
- C. Tamames-Tabar, D. Cunha, E. Imbuluzqueta, F. Ragon, C. Serre, M. J. Blanco-Prieto and P. Horcajada, *J. Mater. Chem. B*, 2014, **2**, 262.
- M. Kim, J. F. Cahill, Y. Su, K. A. Prather and S. M. Cohen, *Chem. Sci.*, 2012, **3**, 126.
- J. H. Cavka, S. Jakobsen, U. Olsbye, N. Guillou, C. Lamberti, S. Bordiga and K. P. Lillerud, *J. Am. Chem. Soc.*, 2008, **130**, 13850.
- S. J. Garibay and S. M. Cohen, *Chem. Commun.*, 2010, **46**, 7700.
- F. Vermoortele, B. Bueken, G. Le Bars, B. Van de Voorde, M. Vandichel, K. Houthoofd, A. Vimont, M. Daturi, M. Waroquier and V. Van Speybroeck, *J. Am. Chem. Soc.*, 2013, **135**, 11465.
- A. Schaate, P. Roy, A. Godt, J. Lippke, F. Waltz, M. Wiebcke and P. Behrens, *Chem.-A Euro. J.*, 2011, **17**, 6643.
- J. Joo, T. Yu, Y. W. Kim, H. M. Park, F. Wu, J. Z. Zhang and T. Hyeon, *J. Am. Chem. Soc.*, 2003, **125**, 6553.
- K. C.-W. Wu, Y. Yamauchi, C.-Y. Hong, Y.-H. Yang, Y.-H. Liang, T. Funatsu and M. Tsunoda, *Chem. Commun.*, 2011, **47**, 5232.
- J. Gu, M. Huang, J. Liu, Y. Li, W. Zhao and J. Shi, *New J. Chem.*, 2012, **36**, 1717.
- P. Horcajada, T. Chalati, C. Serre, B. Gillet, C. Sebrie, T. Baati, J. F. Eubank, D. Heurtaux, P. Clayette, C. Kreuz, *Nat. Mater.*, 2009, **9**, 172.

Table of Contents Entry

Inherent anchorage in UiO-66 nanoparticles for efficient capture of alendronate and its mediated release

An unprecedented alendronate loading capacity was achieved in UiO-66 nanoparticles thanks to the inherent drug anchorages of Zr-O clusters therein.

Xiangyang Zhu, Jinlou Gu,* Yao Wang, Bing Li, Yongsheng Li, Wenru Zhao, and Jianlin Shi*

